



Preparation And Characterization Of Chromium (Cr)- Dopant Tungsten Oxide(WO_3) Nanoparticles For Photocatalytic Applications

G.Thirumoorthi,¹ B.Gnanavel,²

1.PG & Research Department of physics ,Government Arts College (Autonomous),Salem-636 007,Periyar University ,Tamilnadu, India

2. .PG & Research Department of physics, Chikkaiah Naicker College, Erode -638 004,Bharathiar University ,Tamilnadu,,India

ABSTRACT:

The role of chromium (Cr ~ 2 & 5 wt. %) of in WO_3 nano dimensional materials at W site for the same photocatalytic applications prepared by microwave irradiation technique (2.45GHZ, 180 W/10 min). The XRD investigation confirms that the samples ($WO_3.H_2O$) prepared using chromium have formed in the orthorhombic structure. Similarly, the samples prepared without dopant also had the same structure. After annealing at 600°C for 5 hours in ambient atmosphere, dopant free samples have turned out to be stoichiometric tungsten oxide (WO_3). SEM observation showed that the sample annealed at 800°C consisted of well separated elongated structures composed of nanoparticles. Based on optical analysis the band gap energies which were estimated for all the samples indicating dopant free samples have less optical conductivity than the chromium assisted samples. The Absorption characterization results reveal that these prepared samples (5 wt. % doped chromium) are suitable for photo catalytic applications.

Keywords : Tungsten oxide (WO_3) , chromium(Cr) doped, semiconducting metal oxide, photocatalytic activity

1. Introduction

In recent years, Nanoscale materials attracted many fields of specialization because of their novel nature and especially with large surface area. To date, high surface energy-based nano-scale materials are of great interest for a spectrum of applications that includes photocatalysis, chemical sensors, gas sensors biosensors,electrodes in fuel cells, and so forth [1]. In focusing on this special case tungsten oxide(WO_3) are in recent years are considering a peculiar candidate in the fields of smart windows[2], catalysis with photons applications[3], luminescent materials [4], and inthe fabrication of various sensor-based devices for chemical sand gases [5] due to its different polymorphism and deficiency in oxygen along with the growth atmosphere.Moreover, it is to be understood that both the electrical and optical properties of thematerials depend on the dimension and shape at the microscopic level of therespective end products. Hence, the novel materials being fabricated and synthesized for many applications are purely based on their shape and

distributions in particle size during the synthesis process of the nano-scale materials. Moreover, foreign bodies such as dopants have contributed to tuning relatively better shape at the microscopic level and for high surface energies at the nano level. Hence, To date, several synthesis methods are being adopted to synthesize pure and doped tungsten oxide both in the form of a paste, thin films, nanopowders; deposition as vapor [6], a hydrothermal technique [7], and sol-gel technique [8], acidification [9], electrospinning [10], electrodeposition [11], etc. However, the interesting thing belongs to these procedures are cost-effective with high yield. To overcome all these flaws, new synthesis methods are being focused to control the size and morphology in the optimized condition to satisfy certain applications. Recently, researchers are focusing on the synthesis and characterization of pure and metals incorporated nano scale WO_3 for their respective applications. Prepared pure and copper-associated WO_3 nano materials as photonic crystals by the sol-gel templating technique that utilized calculations process to detect volatile organic gases. Their results explored the prepared nano crystals of pure and doped WO_3 replica sensors that had responded more when compared to that pristine ones because of their variation in morphologies [12]. Pure and Zinc doped thin films of WO_3 explored enhanced behavior in both photocurrent and photo-activity [13]. In some of the literature, they Prepared pure and chromium-doped porous tungsten oxide (WO_3) nanoscale material by cost-effective and high-yield chemical precipitation to analyze amines and tetra methyl amines. They proved that the end product had poor sensitivity for NH_3 and TMA [14]. Xia et al. synthesized pure and Au_doped WO_3 nanoscale materials using a simple colloidal chemical method. The obtained results showed that the Au on WO_3 may be a suitable candidate to detect NO_2 cryogenic temperature [15]. Fabrication of pure and "Ti" doped WO_3 films on the Silicon (Si) wafers in (100) direction with the help of a highly efficient sputtering technique resulted in better conductivity for doped samples in an ambient atmosphere than that of pristine samples [16].

2. Materials and Methods

In a typical procedure, Pure and "Cr" (~ 2 & 5 wt.%) doped tungsten oxide (WO_3) nano-dimensional powders were prepared by using the facile microwave irradiation method under ambient conditions. The detailed experimental procedure is as follows: An analytical grade of 4.98 g of tungstic acid (H_2WO_4) was dissolved in 20 mL of sodium hydroxide (NaOH) with a one molar ratio. The resultant yellow-colored solution was stirred for 20 min to get a uniform saturated solution. This resultant yellow-colored hydrated sodium tungstate ($Na_2WO_4 \cdot 2H_2O$) solution was obtained due to the proton exchange protocol process which has been given by the equation below. On the other hand, 2 and 5 wt.% of Chromium Nitrate (Cr_2NO_3) solution was prepared using deionized water and that was mixed along with sodium tungstate solution was stirred for 30 min. Both the solution was mixed slowly together and the final solution was stirred again for 30 min. The pH of the solution was neutral (7.0) and it was tuned up to 1 by adding a few drops of HCl because it may act as a precipitating agent and also a suitable medium for the end products to have specific morphology. In addition to the above solution, 5 ml of double distilled water (~ 50 % of precursor solution) was added to respond to microwave quickly during their radiation process. In the progression, the final solution was transformed into a household microwave oven (2.45GHz and optimum power of 900 W) since microwaves allow the products with controlled shape and size. Moreover, it minimizes the thermal gradients during the synthesis process by manipulating nucleation growth and kinetics. In addition to the above, the difference in microwave extinction coefficient between the solvent and reactant along with the values of dielectric constants and selective dielectric heating rate can provide significant enhancement in the rate of the chemical reaction. By bearing in mind the importance of microwave irradiation (MWI) over conventional

heating methods, the conditions in the microwave oven were set to 240 W for 10 min at room temperature for the synthesis of nano-dimensional particles. A yellow-colored precipitate was obtained after the microwave irradiation process. The resultant powders were in a muffle furnace at 550° C for 6 h in ambient conditions to remove the byproducts and to improve the crystallinity.

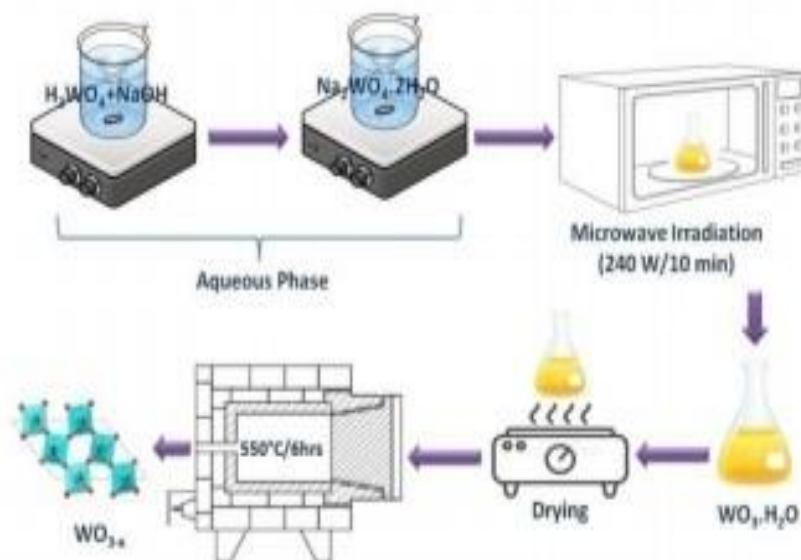


Figure 2.1 .Schematic representation of the preparation by microwave irradiation method

3 Result and Discussion

3.1 Powder XRD analysis

The present result analyzed the respective diffraction pattern for Pristine and metal incorporated as dopants for tungsten anhydride for annealed sample. The Fig. [3.1 (a) & (b)] obtained results showed the formation of the orthorhombic phase of stoichiometric tungsten anhydride with high crystalline nature and also in agreement with JCPDS 43-1035.

A significant trace of change in diffraction pattern observed in the case of the doped sample revealed the presence of dopant as ions in between the lattice site of WO_3 may be due to significant atomic radii of dopant ion. Simultaneously, the contribution of dopants also played a vital role to tune the crystalline nature of the end products as observed in this result .

The corresponding average crystallite size of the prepared samples was calculated from the diffraction pattern for corresponding XRD peaks according to using Scherrer's equation

$$D = K\lambda / \beta \cos\theta$$

Where

D - Average crystallite size (nm)

λ - Wavelength of the X-ray radiation (10^{-10} m)

K - Constant equal to 0.89

β - Full width at half maximum intensity

Θ - Half diffraction angle

The respective lattice parameter for all samples was calculated and they were given a tetragonal system,

$$1/d^2 = (h^2 + k^2 / a^2) + (l^2 / c^2)$$

Where

a, c - Lattice parameters

d - Interplaner angle

The formula helped to calculate the average crystallite size and was also used to understand the role of dopants in the samples calcined at 600°C in an ambient atmosphere with orthorhombic and monoclinic phases which is highly favorable for photo catalytic activity and sensing applications .

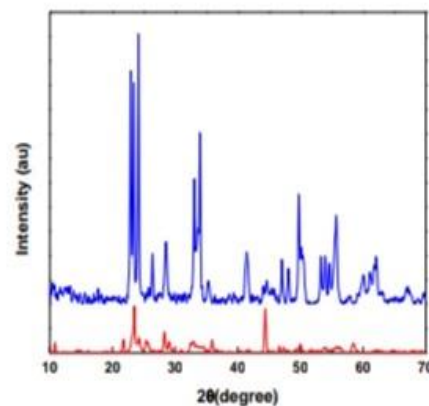


Figure 3.1 (a) WO_3 without doping ,(b) WO_3 with doping

4. UV - VIS - DRS Analysis

The absorption spectra of the prepared end products were obtained and analyzed the reflectance measurement with Kubelka-Munk (KM) absorption function.

$$F(R) = (1 - R_{\infty})^2 / 2R_{\infty}$$

Where

R_{∞} - Reflectance of the sample

F(R) - Corresponding absorbance

Fig. 4.1. (a) shows the UV-VIS absorption spectra of all the prepared samples. The results clearly emphasized a blue shift to calculate the band edge towards the ultraviolet region(UV) upon co-doping. The samples exhibit a very low transparency window at the UV region and the onset of absorption band accurse around the UV and visible region. The results may be due to the charge transfer from the valance band (mainly formed by 2p Orbitals of the Oxide anions and between cation) available in the conduction band .

Fig. 4.2. (b) also shows that the value was obtained from the Kubelka-Munk(KM) absorption plot. The band gap was calculated by using the plot of $(\alpha hv)^2$ vs $h\nu$ which is shown in the figure and was found to be 1.56 eV and 1.98 eV respectively. By assuming that tungsten anhydride has a direct type of transition

$$(\alpha hv) = A (hv - E_g)^n$$

Where,

$h\nu$ - The absorption coefficient

A - Proportionality constant

E_g - Band gap and a constant respectively

n- Type of transition

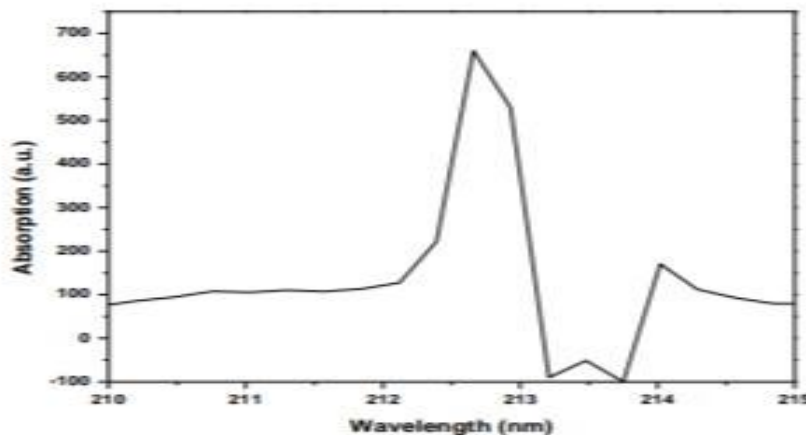


Figure 4.2 (a) WO₃ without doping

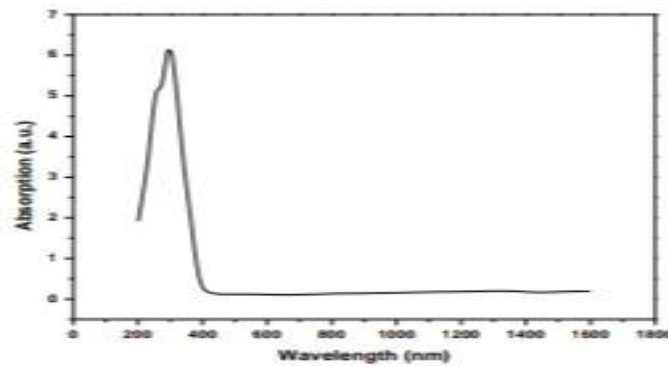


Figure 4.2 (b) .WO₃ with doping

5. Microscope Analysis (FE-SEM)

The microscope analysis were carried out on prepared and annealed nanoparticles of pure and doped tungsten anhydrides on an aluminum substrate are shown in Fig. 5.1(a). This FE – SEM resembles the formation of exact 3D cubic-like morphology with neatly aligned morphology having the dimension of the order of around 1 – 5 μm in long axis and 2 - 5 μm in the shorter axis corresponding to (020) plane which is in agreement with the Powder XRD analysis. Above all the change in morphology arising due to crystallographic shearing stress process transfer between “W” and “O” ions present in the plates that have been marked in Figure.

Fig. 5.1.(b) also exhibited clear morphological nature for doped well-separated WO₃- δ nanoparticles of the order of 2 – 4 μm on the lateral axis and 1 - 2 μm on the longitudinal axis. This may be because the formation of high crystalline nature happened between the particles during the recrystallization process because of the annealing effect. The attainment of a highly uniform with high crystalline nature than the pure sample illustrated the role of dopants in modifying the morphology of the end products especially annealed samples .

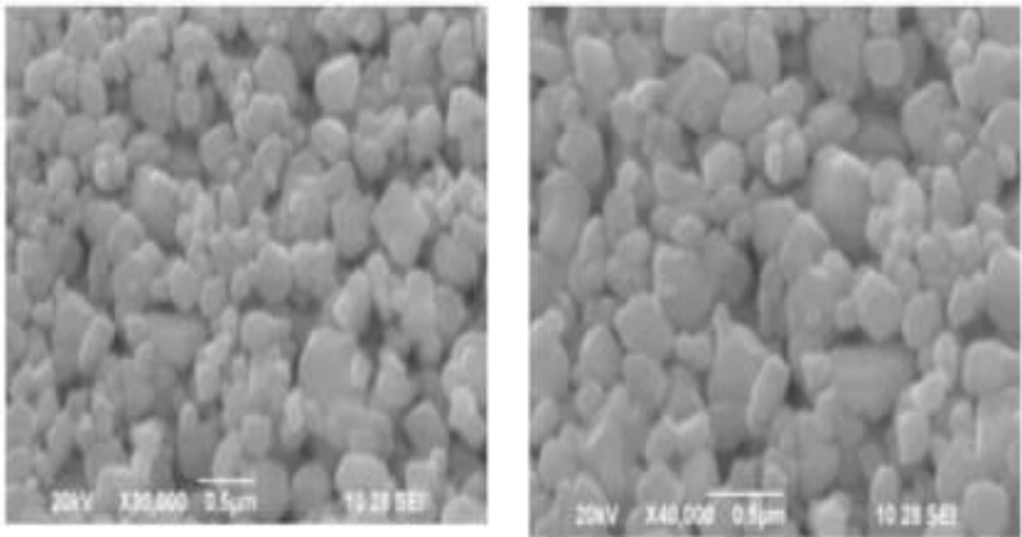


Figure 5.1 (a) .FE-SEM images of pure

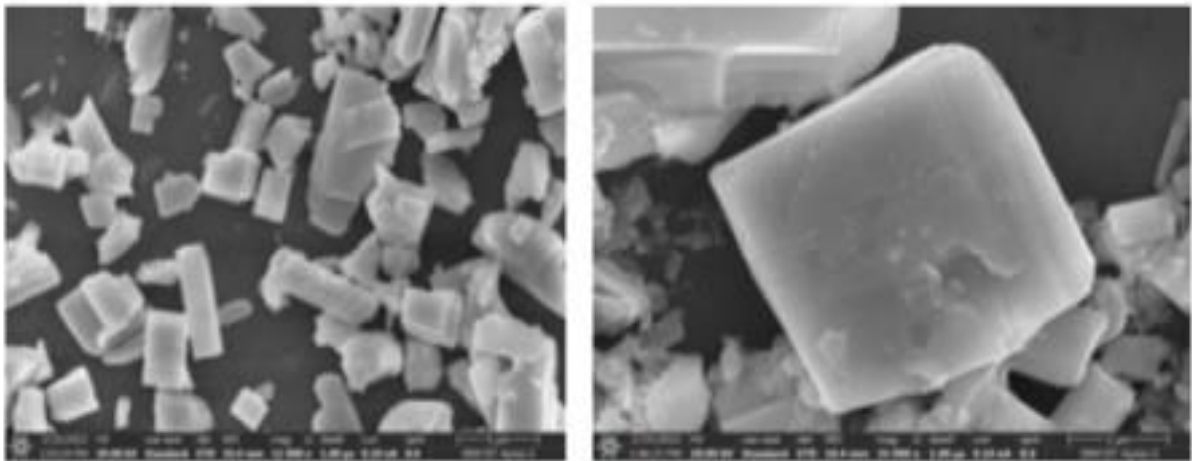
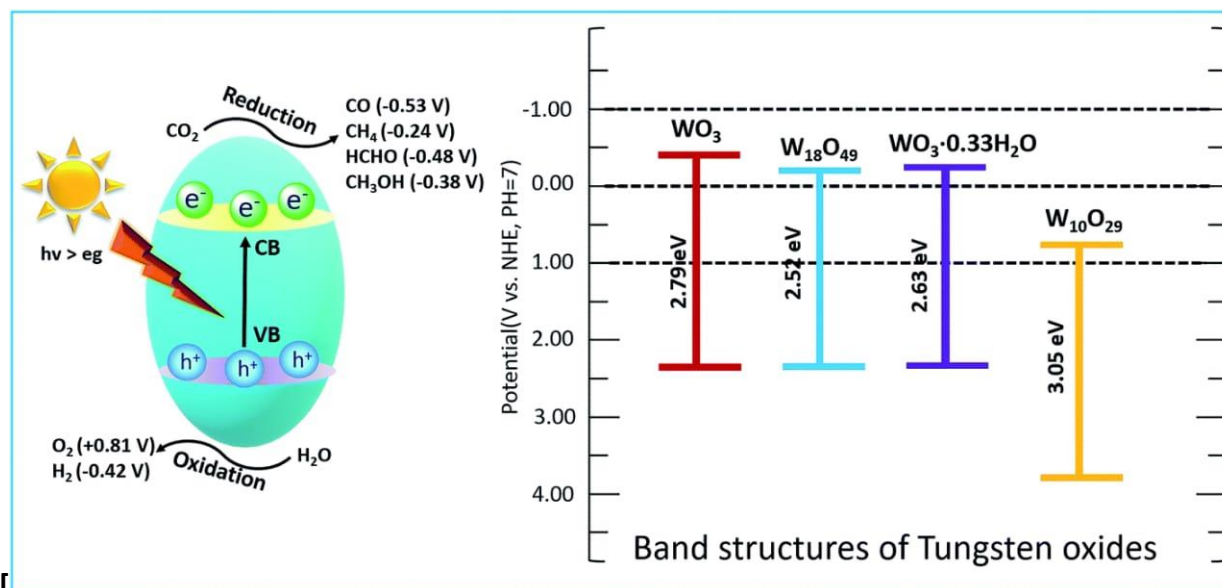


Figure 5.1 (b) .FE-SEM images doped

6. Photocatalytic Activity



The corresponding photo catalytic activity of the prepared nanoparticles was carried out by the photo degradation of Methylene Blue(MB) dye under the illumination of UV light and the corresponding absorption spectra for the tested compound are shown in Fig. 6.1. It revealed that the dye is degrading under the Infrared region(IR). The degradation efficiency of the tested compounds was calculated using the below formula

$$\text{Degradation efficiency\%} = \frac{A_0 - A_t}{A_0} \times 100\%$$

Where

A_0 and A_t are the absorbance at $t = 0$ and corresponding time respectively.

The obtained efficiency was found to be 36.6% due to hydroxyl radical (OH^\bullet) and superoxide radical (O_2^\bullet).

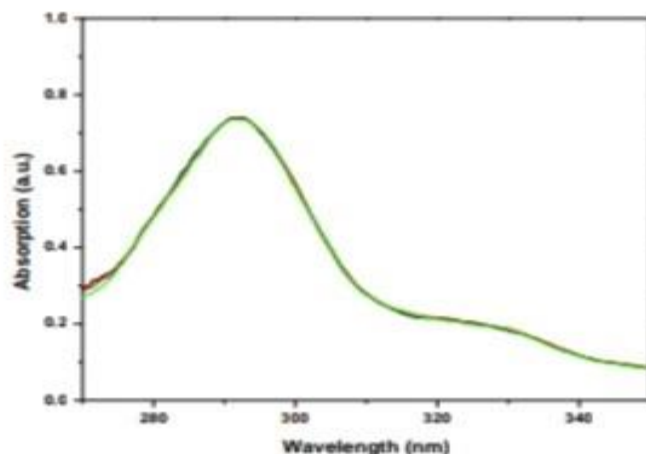


Figure (6.1) UV absorption spectra of prepared silver nanoparticles for Different concentration

7. Conclusions

The work successfully reports the synthesis and characterization of Cr-doped tungsten anhydride nano materials which were prepared using the household microwave irradiation technique for magnetic applications. The corresponding powder diffraction using X-ray as a source confirmed the phase formation of the end products with orthorhombic and monoclinic phases respectively for anhydride and hydride tungsten oxide nano particles in the case of both pure and doped. The corresponding optical properties of the samples from UV-VIS analysis using absorption mode revealed that the oxygen-deficient nature of the samples plays the to tuning band gap energy of the prepared materials and these may lead to photo catalytic applications. The microscopic analysis exhibited the contribution of dopant while changing its morphology during the synthesis process.

References

- [1] C.G. Granqvist (Ed.), Renewable Energy Series: Materials Science for Solar Energy Conversion Systems, Pergamon Press, Oxford, UK, 1991.
- [2] G.A. Niklasson, I. Berggren, A.L. Larsson, Solar Energy Mater. Solar Cells 84 (2004) 315.
- [3] J. Yang, P. K. Dutta, Sensors and Act. B, 136 (2009) 523.
- [4] T. Kida, A. Nishiyama, M. Yuasa, K. Shimano, N. Yamazoe, Sensors and Act. B, (2008).
- [5] F. Jiang, T. Zheng, Y. Yang, J. Nano crys. Solid, 354 (2008) 1290.
- [6] O. U. Nimitrakoolchai, S. Supothina, Mater. Chem and Physics, 112 (2008) 270.
- [7] L. Chen, S. C. Tsang, Sensors and Act. B, 89 (2003) 68.
- [8] T. Siciliano, A. Tepore, G. Micocci, A. Serra, D. Manno, E. Filippo, Sensors and Act. B, 133 (2008) 321.
- [9] G. Leftheriotis, P. Yianoulis, Solid State Ionics, 179 (2008) 2192.
- [10] Y. c. Nah, A. Ghicov, D. Kim, P. Schmuki, Electrochemistry Communications, 10 (2008) 1777.
- [11] L. Guo, G. Gao, X. Liu, F. Liu, Materials Chemistry and Physics 111 (2008) 322.
- [12] A. Sadeghzadeh-Attar, M. SasaniGhamsari, F. Hajiesmaeilbaigi, Sh. Mirdamadi, Quantum Electronics & Optoelectronics, 10 (2007) 36.
- [13] C. M. Carney, S. Yoo, S. A. Akbar, Sensors and Act. B, 108 (2005) 29.
- [14] Y. Li, H. Li, T.Li, G. Li, R. Cai, Microporous and Mesoporous Materials, 117 (2009) 444.
- [15] Y. H. Liae, J.C. Chou, Materials Chemistry and Physics, (2008), DOI: 10.1016.
- [16] G. V. Kunte, U. Ail, S. H. Shivakumar, A.M. Umarji, Bull. Mater. Sci., 28 (2005) 243.

[17] K. J. Lethy, D. Beena, R. Vinodkumar, V.P. Mahadevan Pillai, V. Ganesan, V. Sathe, D.M. Phase, Appl. Phys. A, 91 (2008) 637.

[18] C. S. Rout, K. Ganesh, A. Govindaraj, C.N.R.Rao, Appl. Phys. A, 85 (2006) 241.

[19] O.M. Hussain, A. S. Swapnasmitha, J. Jhon, R. Pinto, Appl. Phys. A, 81 (2005) 1291.

[20] R.Vinu, G. Madras, Applied Catalysis A: General, 366 (2009) 130.

[21] N.Venkatachalam, M.Palanichamy, B. Arabindoo, V.Murugesan, Jour. Molecular Catalysis A: Chemical, 266 (2007) 158.

[22] P.K.Khanna, N. Singh, S. Charan, Materials Letters, 61 (2007) 4725. [23] N. Rajalakshmi, N. Lakshmi, K.S. Dhathathreyan, International Journal Hydrogen Energy, 33 (2008) 7521.

